

CONF-941129--13

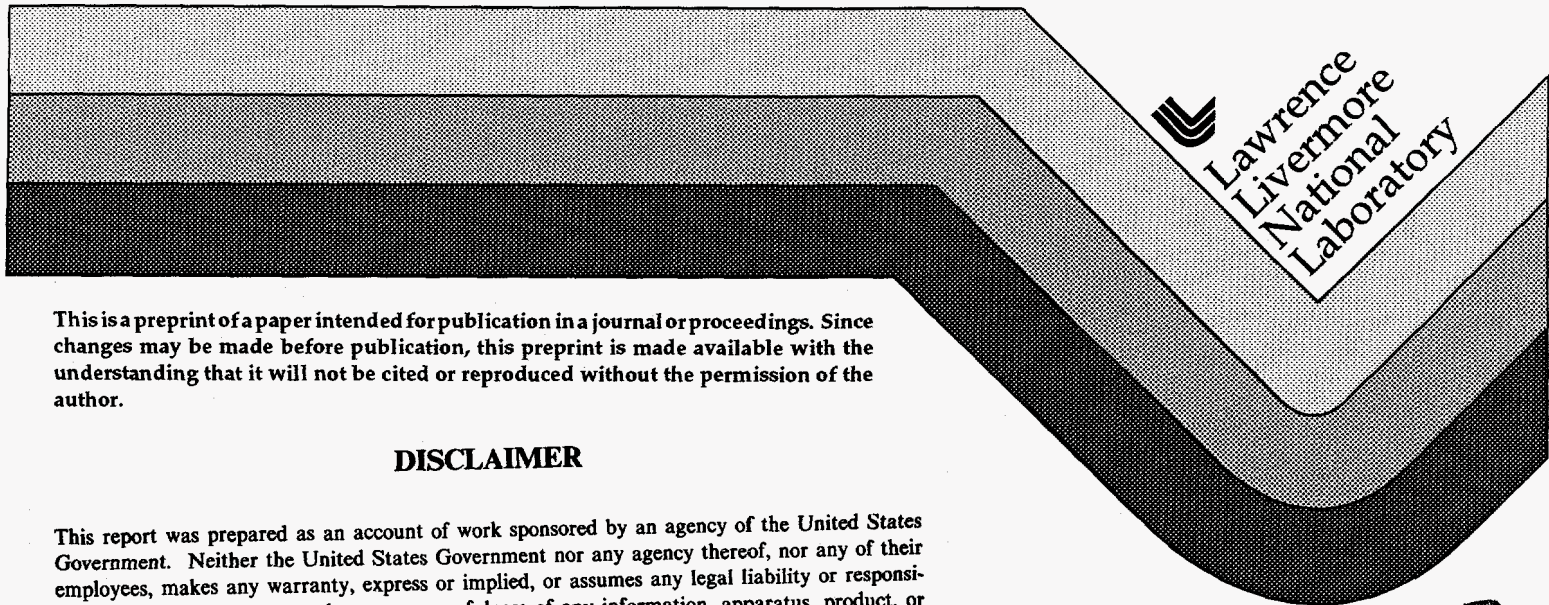
UCRL-JC-118859
PREPRINT

PXAMS--Projectile X-ray AMS: X-ray Yields and Applications

J.E. McAninch, G.S. Bench, S.P.H.T. Freeman, M.L. Roberts,
J.R. Southon, J.S. Vogel and I.D. Proctor
Lawrence Livermore National Laboratory
Livermore, CA 94550 USA

This paper was prepared for submittal to the
*13th International Conference on the
Application of Accelerators in
Research and Industry*
Denton, TX
November 7-10, 1994

October 7, 1994



This is a preprint of a paper intended for publication in a journal or proceedings. Since changes may be made before publication, this preprint is made available with the understanding that it will not be cited or reproduced without the permission of the author.

DISCLAIMER

This report was prepared as an account of work sponsored by an agency of the United States Government. Neither the United States Government nor any agency thereof, nor any of their employees, makes any warranty, express or implied, or assumes any legal liability or responsibility for the accuracy, completeness, or usefulness of any information, apparatus, product, or process disclosed, or represents that its use would not infringe privately owned rights. Reference herein to any specific commercial product, process, or service by trade name, trademark, manufacturer, or otherwise does not necessarily constitute or imply its endorsement, recommendation, or favoring by the United States Government or any agency thereof. The views and opinions of authors expressed herein do not necessarily state or reflect those of the United States Government or any agency thereof.

UNCLASSIFIED AND UNLIMITED

MASTER



LL

DISCLAIMER

This document was prepared as an account of work sponsored by an agency of the United States Government. Neither the United States Government nor the University of California nor any of their employees, makes any warranty, express or implied, or assumes any legal liability or responsibility for the accuracy, completeness, or usefulness of any information, apparatus, product, or process disclosed, or represents that its use would not infringe privately owned rights. Reference herein to any specific commercial products, process, or service by trade name, trademark, manufacturer, or otherwise, does not necessarily constitute or imply its endorsement, recommendation, or favoring by the United States Government or the University of California. The views and opinions of authors expressed herein do not necessarily state or reflect those of the United States Government or the University of California, and shall not be used for advertising or product endorsement purposes.

DISCLAIMER

Portions of this document may be illegible in electronic image products. Images are produced from the best available original document.

PXAMS—Projectile X ray AMS: x ray yields and applications*

J.E. McAninch[†], G.S. Bench, S.P.H.T. Freeman, M.L. Roberts, J.R. Southon, J.S. Vogel and I.D. Proctor

Center for Accelerator Mass Spectrometry, Lawrence Livermore National Laboratory, Livermore, California, 94551-9900, USA

*This work performed under the auspices of the U.S. Department of Energy by Lawrence Livermore National Laboratory under contract W-7405-Eng-48.

[†]Corresponding author. Electronic mail: mcaninch1@llnl.gov.

Abstract

Characteristic x rays have recently been explored as a method for the detection and identification of ions in accelerator mass spectrometry (AMS) [H. Artigalas *et al.*, Nucl. Inst. and Meth. B 92, 227 (1994); M. Wagner *et al.*, Nucl. Inst. and Meth. B 89, 266 (1994)]. After analysis in the AMS spectrometer, the ions stop in an appropriately chosen target and the induced x rays identify the ions by atomic number. For the application of AMS to higher mass isotopes, characteristic x rays allow significantly better discrimination of competing atomic isobars than is possible using energy loss detectors. Characteristic x rays also show promise as a convenient component in hybrid detection systems. Measurements of x ray yields are presented for Si, Fe, Ni, Se, Mo, and Pd ions of 0.5-2 MeV/AMU. The yields rise by more than a factor of 10 over this energy range, and approach 1 x ray per incident ion at 2 MeV/AMU for the lighter ions. Preliminary work on the application of PXAMS to the detection of ⁷⁹Se is described.

1. Introduction

Stable atomic isobars are the dominant background limiting the sensitivity of accelerator mass spectrometry (AMS) for most isotopes. For isotopes of atomic number $Z \lesssim 20$, the post-spectrometer rejection of these backgrounds relies on the energy loss of ions in matter. The rate of energy loss dE/dx is a function of Z . It is therefore possible to distinguish isobars by sampling the energy deposited at different depths in the material. The standard AMS detector is the multiple anode gas counter, in which the ionization of a low pressure (50-200 Torr) gas is used as a measure of energy deposition. The $\Delta E - E$ telescope using silicon surface barrier detectors is similar. Another alternative is the gas-filled magnet, in which a magnetic field combines with energy loss and charge changing interactions to physically separate the isobars.

Isobar rejection techniques that rely on energy loss suffer from two intrinsic features of the energy loss process — charge changing interactions and the statistical nature of multiple collisions — which cause the width of the energy distribution to increase as the ions slow down. At lower Z this spreading, known as energy straggling, is small compared to the difference in energy loss between isobars. With increasing atomic number, the straggling increases relative to the energy loss difference, so that isobar separation becomes progressively less effective, and at some point unworkable. For the energies accessible with larger tandem accelerators, this point is somewhere in the range $Z \approx 25 - 30$.

Recently, two groups have explored an alternative method for isobar rejection which does not rely on energy loss. In this method, a variant of PIXE, projectile ions are identified by the characteristic x rays they emit when slowing down in matter. These x rays are of atomic origin, and can therefore be used to distinguish the ions by atomic number. Artigas *et al.* [1,2] examined this approach for the AMS detection of ^{36}Cl , ^{59}Ni , and ^{94}Nb at 15-21 MeV, and Wagner *et al.* [3] explored its application in the detection of ^{59}Ni and ^{60}Fe at 55 MeV. In both works, the purpose was to find a method for detecting the radioisotopes given the constraints of the available accelerators.

We have begun to examine the applicability of this technique, which we are referring to as

PXAMS (Projectile X ray AMS), to the detection of several isotopes at Lawrence Livermore National Laboratory (LLNL). In our first exploratory work, we measured the x ray yield vs. energy for ^{80}Se ions stopped in a thick Y target. These results, shown in Fig. 1, demonstrated that useful detection efficiencies could be obtained for Se ions at energies accessible with our accelerator, and that the count rate from target x rays is small compared to the Se $K\alpha$ rate. We followed these measurements with a survey of x ray yields for $Z = 14 - 46$. In this paper we present the results of our x ray yield measurements, describe the experimental arrangement currently used for PXAMS at LLNL, and discuss our preliminary work on the detection of ^{79}Se and other isotopes.

2. Measurement of the x ray yields

X ray yields were measured using the 10 MV FN tandem accelerator [4] at the Center for Accelerator Mass Spectrometry (CAMS) at LLNL. Picoamp currents of selected ions were stopped in thick targets, and the resulting x rays were detected with a lithium-drifted silicon detector (Si(Li)) normally used for PIXE analyses. The Si(Li) detector was placed at 90° to the incident beam, and the target was oriented at 45° .

The number of incident ions was determined by collecting the charge deposited on the targets, which were mostly elemental metal foils of 10 mg/cm^2 thickness or greater. Non-conducting targets (Ge and CaCO_3) were coated with a thin layer of graphite to aid charge collection. Electron suppression was provided by a Faraday cage, biased to +300 V and in electrical contact with the target. The accuracy of the charge collection ($< 10\%$) was measured in three ways: comparison to the currents measured in a proper Faraday cup located behind the target; inter-comparison of the currents measured on different targets; and comparison of the x ray yields for repeat measurements in which the current was changed by more than a factor of 10.

Absolute x ray detection efficiencies were measured using thin ($\sim 50\ \mu\text{g/cm}^2$) PIXE standards. In general, the uncertainties in the measured $K\alpha$ yields were insignificant compared to the $\sim 10\%$ uncertainty in the charge integration. For the $K\beta$ yields, the uncertainties were somewhat larger because of increased statistical uncertainty and increased uncertainty in the peak extraction.

The reported yields have not been corrected for attenuation in the target. This systematic effect can be significant in some cases, particularly at higher energies where the ranges are longer, or when the x ray energy is close to a critical absorption edge in the target. As an example, in the measurement of ^{80}Se on an Y target at 100 MeV, we estimate that this effect decreases the measured yield by approximately 7%. This systematic effect does not alter conclusions about the feasibility of PXAMS or the choice of targets.

Results of the yield measurements vs. ion energy for Ni and Se ions are shown in Figs. 1 and 2. The Ni results exhibit a trend similar to the Se results, but with significantly higher yields for the same energy per unit mass. Also seen in Fig. 2 is the good agreement of the present Ni data to the x ray yields of Ref. 2.

Projectile and target yields for Se ions on various targets are displayed in Fig. 3. The optimum target is either Y or Zr, and the shape of the yield curves is essentially the same for different energies (compare the 80 and 100 MeV results). The projectile and target $K\alpha$ yield curves illustrate the cross-section resonances which results from the formation of molecular orbitals between the projectile and target atoms when there is an energy overlap between the respective K shells. This atomic physics phenomenon has been studied in detail by Meyerhof *et al.* [5], and the present data follow the trends in that reference. In addition, we studied the second resonance region (near $Z=80$), in which there is an overlap between the projectile K shell and the target L shell. The maximum yield in the second resonance region is about 75% of the Y yield, however this is probably not a useful region for PXAMS because of the intensity and number of target $L\alpha$ lines.

In Table 1, we present additional measured yields which are representative of the efficiencies that will be accessible with our accelerator. Yields as high as 1 x ray per incident ion are accessible for light ions such as Si. The yields are significantly reduced for heavier ions, primarily because of the reduced energy per unit mass. However, even for ^{107}Pd ions, where the best yield is less than 1 x ray per 300 incident ions, we expect that PXAMS will allow more sensitive detection than is possible with other techniques.

We have also examined the use of projectile $L\alpha$ lines, which have significantly higher yields,

however with standard x ray detectors these lines are not resolved from the target $L\alpha$ lines. Spectrum fitting is an option, however this would likely require significant intervention and analysis time per sample on the part of the experimenter. We have considered the possibility of detecting $L\alpha$ lines using a wavelength dispersive x ray detector, which could provide increased isobar rejection, but the small acceptance of these detectors is expected to be a significant drawback [6].

3. PXAMS at LLNL

For further PXAMS development, we have purchased a high resolution high-purity germanium (HPGe) detector[†] and have begun preliminary measurements on the AMS beamline at CAMS. A schematic of our setup is shown in Fig. 4. The target and absorbers are placed immediately in front of the Be window of the detector. This design was chosen to maximize the solid angle intercepted by the detector. While the solid angle in this geometry could in principle approach 2π , the solid angle at present is about half this value because of the ~ 5 mm distance between the crystal and the Be window.

The 0° detector position leads to significant shifting and broadening of the x ray lines due to Doppler shifts. A somewhat smaller effect (which acts at all angles) is the shifting of the atomic levels caused by the high average charge state of the ions as they slow down in the target. Because of the Doppler broadening, a careful choice of target thickness and accepted angular range is important to find a balance between maximizing the x ray yield and minimizing the width of the peaks to improve for isobar rejection.

We have begun development of PXAMS for the long-lived radioisotope ^{79}Se , which could not previously be measured by AMS because of background from the stable isobar ^{79}Br . ^{79}Se is interesting as a tracer in the study of selenium biochemistry and the metabolism of selenium compounds, and as a component of radioactive wastes. In addition, it has recently been noted that the accepted half-life of ^{79}Se may be in error by as much as an order of magnitude [7]. This

[†] An Igleet-X detector, 100 mm^2 active area and 145 eV FWHM resolution at 5.9 keV, purchased from EG&G Ortec, Oak Ridge, TN.

uncertainty has implications in reactor-irradiated fuel composition and in radioactive waste management, and a new measurement has been called for in the literature [8]. As part of our future plans, we propose to re-measure the ^{79}Se half-life using AMS.

Spectra taken with a natural Se sample are shown in Fig. 5. For these spectra, the ion detection efficiency was $\sim 5 \times 10^{-3}$. The ^{79}Br $K\alpha$ peak indicates a $^{79}\text{Br}/^{78}\text{Se}$ in the sample of $\sim 1 \times 10^{-6}$. The ^{79}Br counts which lie in the Se $K\alpha$ region represent a background $^{79}\text{Se}/^{78}\text{Se}$ ratio of $\sim 2 \times 10^{-8}$. A planned modification of the detector will reduce the low energy tailing by a factor of 6, leading to an isobar rejection of 300. We are currently exploring chemical separation techniques to further lower the ^{79}Br background.

We have also begun to explore PXAMS for the isotopes ^{41}Ca [9], ^{60}Fe , ^{59}Ni , and ^{63}Ni , and will be pursuing other isotopes up to $Z \approx 50$, depending on the interest and the prospects for sample preparation and negative ion production.

Further improvements to our PXAMS capabilities will involve the combination of PXAMS with other detection methods in a hybrid system. A TOF detector exists in the AMS beamline [10] which will allow rejection of some backgrounds, mostly from stable isotopes of the isotope of interest. These backgrounds will also be reduced by the addition of new ion source with a spherical electrostatic analyzer. Certain backgrounds could also be removed by combining PXAMS with a silicon surface barrier detector placed behind a thin target foil. This could be done for instance either with a ΔE detector placed between the target and x ray detector, albeit with a factor of 5-10 decrease in efficiency.

In summary, the results reported here demonstrate that characteristic x rays can provide an effective tool for the detection and identification of ions in AMS. The reduced detection efficiency is adequately offset by the gains in isobar rejection and simplicity of design.

Acknowledgments

The authors gratefully acknowledge financial support from the US DOE Office of Non-Proliferation and National Security.

REFERENCES

- [1] H. Artigalas, M.F. Barthe, J. Gomez, J.L. Debrun, L. Kilius, X.L. Zhao, A.E. Litherland, J.L. Pinault, Ch. Fouillac, P. Caravatti, G. Kruppa and C. Maggiore, Nucl. Inst. and Meth. B 79, 617 (1993).
- [2] H. Artigalas, J.L. Debrun, L. Kilius, X.L. Zhao, A.E. Litherland, J.L. Pinault, C. Fouillac and C. Maggiore, Nucl. Inst. and Meth. B 92, 227 (1994).
- [3] M.J.M. Wagner, H. Synal and M. Suter, Nucl. Inst. and Meth. B 89, 266 (1994).
- [4] J.R. Southon, M.W. Caffee, J.C. Davis, T.L. Moore, I.D. Proctor, B. Schumacher and J.S. Vogel, NIM B 52, 301 (1990).
- [5] W.E. Meyerhof, R. Anholt, T.K. Saylor, S.M. Lazarus and A. Little, Phys. Rev. A5, 1653 (1976).
- [6] D. Morse, G.S. Bench, A. Pontau, and S.P.H.T. Freeman, these proceedings.
- [7] O.W. Hermann, private communication (1994).
- [8] B. Singh, Nucl. Data Sheets 70, 437 (1993).
- [9] S.P.H.T. Freeman, R.E. Serfass, J.C. King, J.R. Southon, Y. Fang, L.R. Woodhouse, G.S. Bench and J.E. McAninch, these proceedings.
- [10] I.D. Proctor, J.R. Southon and M.L. Roberts, Nucl. Inst. and Meth. B 92, 92 (1994).

TABLE I. Representative measured x ray yields for various ions and targets.

Isotope	Half-Life (y)	Competing Isobar	Measured Ion	Target	Energy (MeV)	K α x rays per incident ion
³² Si	100	³² S (Z+2)	²⁸ Si 7+	CaCO ₃	56	1.0
				Ti	56	0.3
⁶⁰ Fe	1.5×10 ⁶	⁶⁰ Ni (Z+2)	⁵⁶ Fe 11+	Cu	102	0.8
⁵⁹ Ni	8×10 ⁴	⁵⁹ Co (Z-1)	⁵⁸ Ni 11+	Zn	102	0.5
				Ge	102	0.4
⁷⁹ Se	~10 ⁵ -10 ⁶	⁷⁹ Br (Z+1)	⁸⁰ Se 10+	Y	100	0.05
				Y	120	0.08
⁹³ Mo	4×10 ³	⁹³ Nb (Z-1)	⁹² Mo 11+	Rh	106	0.008
¹⁰⁷ Pd	7×10 ⁶	¹⁰⁷ Ag (Z+1)	¹⁰⁶ Pd 11+	Ag	106	0.003

FIGURE CAPTIONS

FIG. 1. X ray yields vs. incident ion energy for ^{80}Se ions on a thick Y target. Shown are the Se $K\alpha$ (squares) and $K\beta$ (diamonds) yields, and the Y $K\alpha$ yields (crosses). For the $K\alpha$ yields, error bars are smaller than the symbols. The curves are guides to the eye.

FIG. 2. X ray yields vs. incident ion energy for ^{58}Ni ions on a thick Zn target. Shown are the Ni (squares) and Zn (crosses) $K\alpha$ yields of the present work, and the Ni (inverted triangles) $K\alpha$ yields of Ref. 2. For the present data, error bars are smaller than the symbols. The curves are guides to the eye.

FIG. 3. X ray yields vs. target atomic number for 80 and 100 MeV ^{80}Se ions. Shown are the Se $K\alpha$ yields at 80 MeV (squares) and 100 MeV (open triangles). Also shown for 80 MeV are the Se $K\beta$ yields (diamonds), and the Y $K\alpha$ (crosses) and $L\alpha$ (plusses) yields. For the $K\alpha$ and $L\alpha$ yields, error bars are smaller than the symbols. The curves are guides to the eye.

FIG. 4. Sketch of the PXAMS setup in use at LLNL. Following analysis in the AMS spectrometer, the ions are incident on a target foil. The induced x rays are detected with a HPGe detector. Additional absorbers (Be and mylar) are included to stop the ions and to attenuate low energy x rays.

FIG. 5. ^{79}Se PXAMS x ray spectra for a natural Se sample. 99 MeV $10+$ ions were incident on a 2.0 mg/cm^2 Zr target. The bold spectrum (labeled "mass 79") shows the contamination from the stable isobar ^{79}Br . For the second spectrum (labeled "mass 78"), the low-energy spectrometer was set to inject ^{78}Se to demonstrate the position of the Se x rays. The "mass 78" spectrum has been scaled to approximate a 10:1 $^{79}\text{Br}/^{79}\text{Se}$ ratio in the sample. The peak at $\sim 10\text{keV}$ is from a contaminant in the target.

Fig.1, McAninch, et al, "PXAMS — Projectile X-ray AMS..."

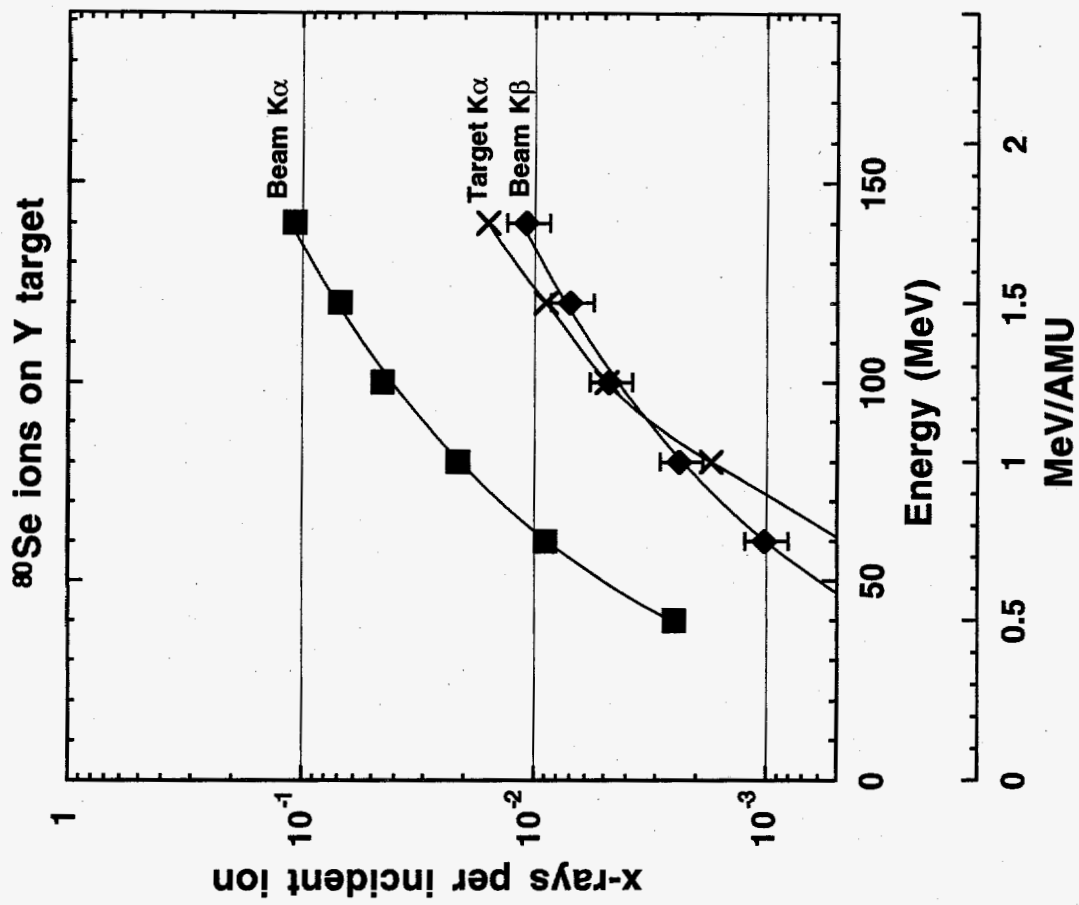


Fig. 2. McAninch, et al, "PXAMS — Projectile X-ray AMS:..."

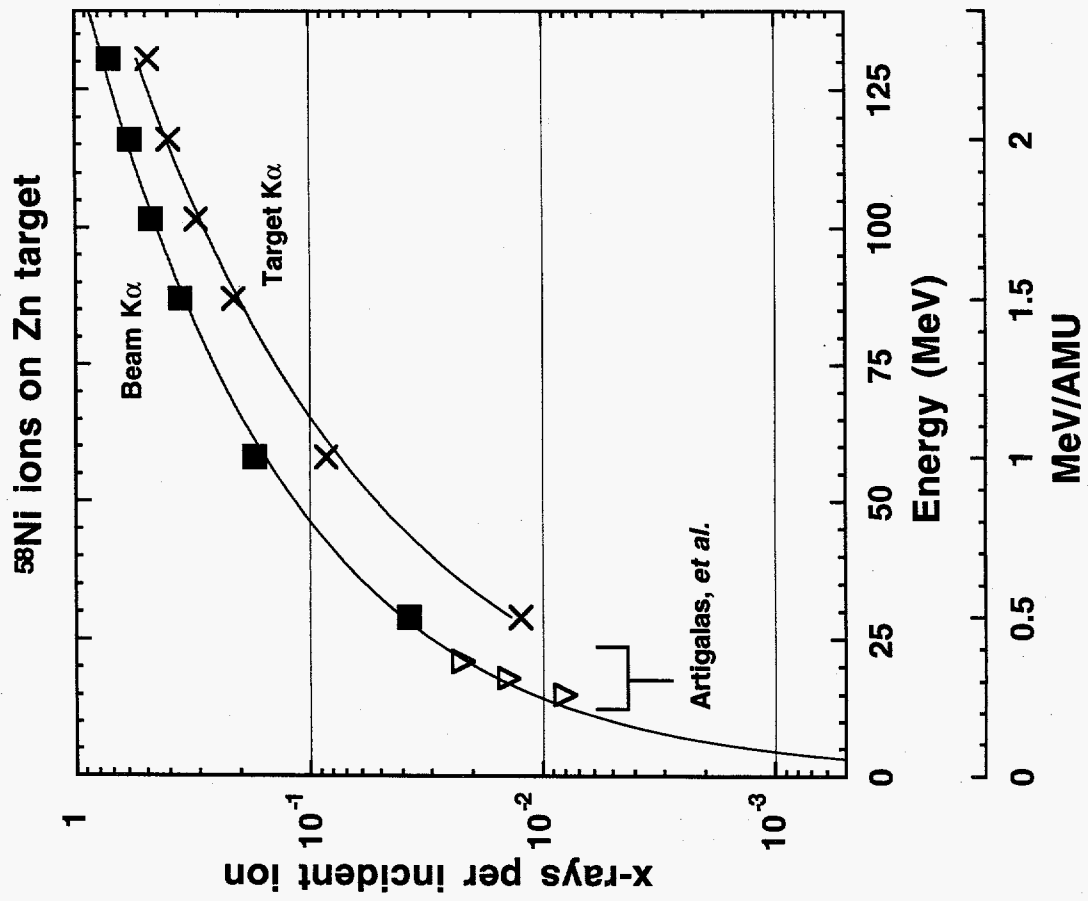


Fig. 3, McAninch, et al, "PXAMS — Projectile X-ray AMS:..."

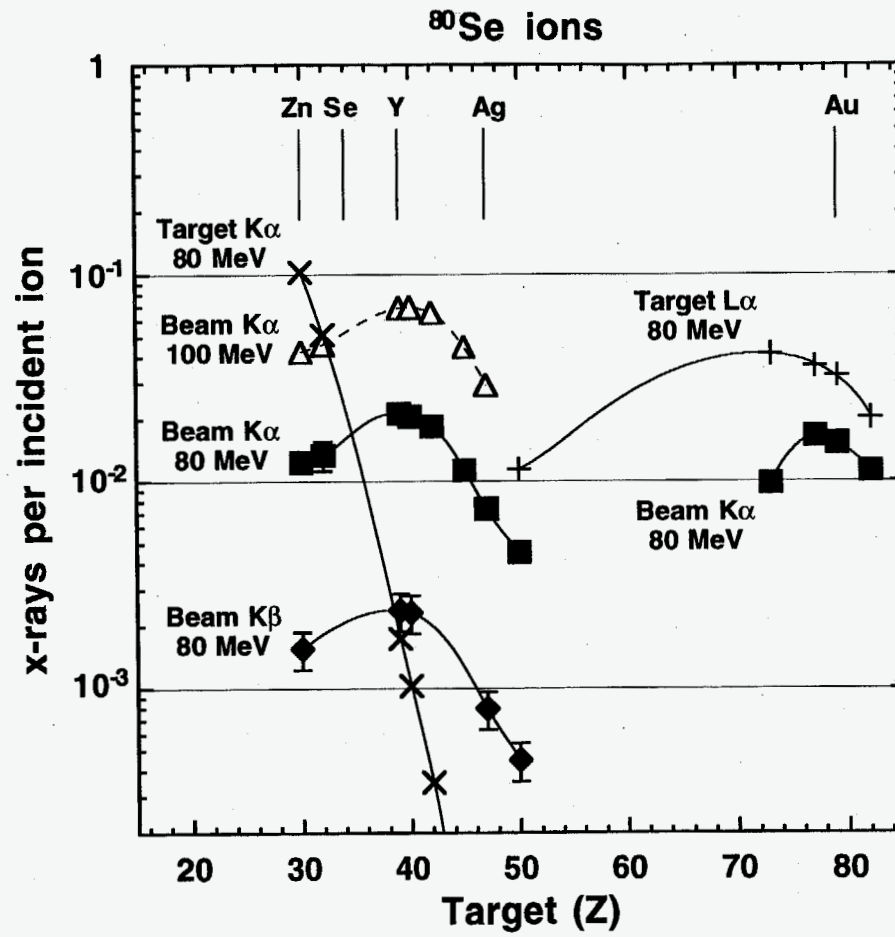


Fig. 4, McAninch, et al., PXAMS - Projectile X ray AMS...

**PXAMS: Projectile X ray AMS
detection and identification of AMS
beams via characteristic x rays**

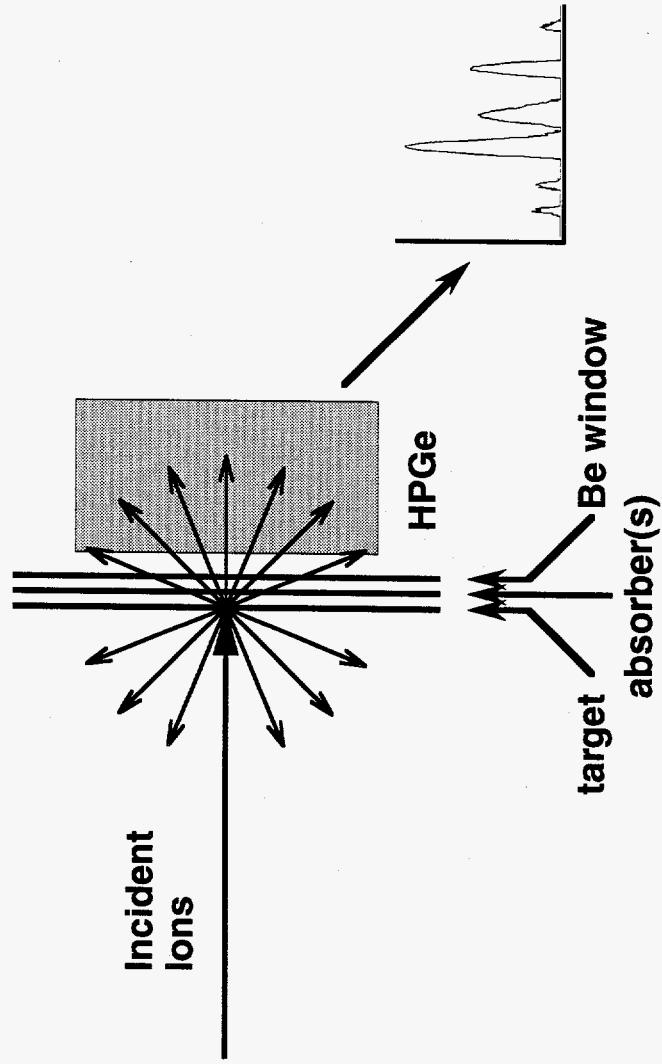


Fig. 5, McAninch, et al, "PXAMS — Projectile X-ray AMS..."

